Int. J. Nanosci. Nanotechnol., Vol. 16, No. 2, June 2020, pp. 91-102

Comparison of Binary and Ternary Compositions of Ni-Co-Cu Oxides/VACNTs Electrodes for Energy Storage Devices with Excellent Capacitive Behaviour

Seied Ali Hosseini[1,*], Morteza Saghafi[2] and Hamed Abiri[3]

[1]Department of Electrical Engineering, Faculty of Engineering, Imam Khomeini International University, Qazvin, Iran.
[2]Department of Materials Science and Engineering, Faculty of Engineering, Imam Khomeini International University, Qazvin, Iran.
[3]Department of Electrical Engineering, Faculty of Engineering, University of Tehran, Tehran, Iran.

*Corresponding author: sahosseini@eng.ikiu.ac.ir
(Received: 03 March 2019 and Accepted: 15 January 2020)

Abstract

Electrochemical performance of binary and ternary oxides composed of Ni, Co and Cu produced over a 3-dimensional substrate of vertically aligned carbon nano-tubes (VACNT) as electrodes for aqueous energy sources, is reported and compared in this paper. VACNTs were fabricated inside a DC-plasma enhanced chemical vapor deposition chamber and composite materials fabricated by thermal decomposition method on the surface of VACNT electrodes. XRD, Raman and electron microscopy tests were used to verify electrodes proper composition and interface between the electrodes substrate and active material. Cyclo-voltammetry experiments were done over electrodes and Co-Cu oxide/VACNT electrode found to have the highest charge capacity of 230 mC cm^{-2} among the electrodes. Electrical impedance spectroscopy was done to determine electrodes electrical behavior in different frequencies and find their characteristics quality as well.

Keywords: *Carbon nanotubes, Composite materials, Energy Storages, Electrical properties*.

1. INRODUCTION

Various kinds of energy storage devices have been developed such as high power aqueous batteries and supercapacitors for a wide range of applications such as internet of things [1-3]. While properties like weight and size were of interest in portable batteries, location - dependent batteries concerns are more about durability, output power, low delay and cost as in traditional electric grids, batteries suffer from poor performance and need large maintenance budgets [4]. Metal oxides are proposed as electrodes materials for batteries [5-7] or supercapacitors [8-13]. Electrodes morphology and composite materials play a significant role in energy devices performance enhancement. Co, Ni and Cu oxides in different shapes and scales have been produced for quality electrodes by many researchers such as CuO hollow spheres prepared for sodium ion batteries which could deliver a reversible capacity of 612 mAh g^{-1} [14].

Moosavifard could store 61.2 C g^{-1} of electrical charges on CuO nanorods fabricated over carbon nanofibers in a potential window of 0.4 V in current densities as high as 50 A g^{-1} proposing them for powerful

supercapacitors [15]. Vinu et al. homogenously loaded nanoporous carbon electrodes with copper oxide nanoparticles by a hard templating approach and achieved a maximum capacity of 300 F g^{-1} for the electrodes at a scan rate of 20 mV s^{-1} [16].
Hue et al coated carbon nanofibers by binary oxides composite of Ni and Co in electrospinning procedure followed by thermal treatment for high-performance energy storages. They could store 836 C g^{-1} electrical charges at 5 A g^{-1} with excellent cycling ability with 80.9% retention after 2000 cycles [5]. Porous Ni-Co Oxide nanorods were fabricated using a solvothermal method followed by thermal decomposition. The specific surface area was increased due to nano-rods one-dimensional morphology and the added porosity. As a result, a rather high capacitance of 600 F g^{-1} was obtained beside a high retention capacity of 80% over 1500 cycles at a constant 5 A g^{-1} current [17]. Cheng et al. also used the same composite but with a flower like morphology to produce charge storage devices. They found that a Ni-Co with a 7:3 molar ratio could have the highest charge storage capacity of 992 C in a potential range of -0.1 to 0.45 V [18]. We also had coated a Ni-Co oxide layer over a vertically aligned carbon nanotube covered substrate to enhance the charge storage capacity of electrodes to 578 C in 0.55 V and 1 mA cm^{-1} [19]. In addition to morphology, material composites provide more opportunities to increase the energy storage devices capacity [20].

Various combination of Co, Cu and Ni binary oxides were studied to store electrical charges. For example, Sui et al. produced Co-Cu oxide electrodes with 100% capacity retention after 1000 cycles with a capacity of 0.189 F g^{-1} at 0.9 V and 5 mA cm^{-2} constant current [21]. Ni oxide nanoparticles deposited on CNTs electrochemical properties were boosted by only 5% of Co dopant ions which yielded 1231 F g^{-1} at 1 A g^{-1} in a report published by Hou and et al [22]. Park et al. reported charge capacity of 178 C g^{-1} at the scan rate and potential of 10 mV s^{-1} and 0.6 V respectively in copper/ nickel oxide electrodes prepared through electroplating, chemical oxidation, and annealing procedure. Electrochemical performance of electrodes was enhanced due to their novel architecture and low contact electrical resistance between copper and nickel layers [23]. Superior rate capability and excellent durability were observed in Co-Cu oxide electrodes by Ezema et al. due to the enhanced redox behavior at nanoporous electrodes. The optimum achieved capacity was 919 C g^{-1} in 1 V potential at 5 mV s^{-1} scan rate for Co-Cu film over an ITO substrate [24]. Synergetic effect between Ni and Cu caused great electrochemical performance to store charges and a high specific capacity of 855 C g^{-1} at 5 A g^{-1} discharge current and a potential range of 0.5 V was recorded for this energy storage device [25]. Zhang et al formed mesoporous nanosheets of Co and Ni oxides by electrochemical deposition that could store 2517 C g^{-1} in a potential window and current of 1 V and 1 A g^{-1} respectively [26].

Zhang et al. also reported capacity properties of the spinel Ni-Co-Cu supported by hybrid reduced graphene oxide nanosheets. A high charge capacity of 646 C g^{-1} was obtained at 1 A g^{-1} [27]. Various electrolytes effects were investigated for a composite electrode made out of Mn, Cu and Co oxides and a large capacity of 7404 F g^{-1}¬ at 20 A g^{-1} in mix KOH/0.04 M K3Fe(CN)6 electrolyte was obtained by Rusi [28]. Micheal also published results for spinel Ni-Co-Cu electrodes indicating charge storage enhancement compared to pristine counterpart Ni-Co oxides. Nanoplatelet shaped Ni-Co-Cu oxides had up to 458 C g^{-1} capacity for electrical charges in 1 V potential [29].

Several methods for composite oxides formation are reported including thermal decomposition and microwave-assisted synthesis [20, 30]. Here we produced them by thermal decomposition and compared electrochemical properties of ternary Ni-Co-Cu oxides with their three different binary combinations of them in similar conditions where they were coated over n-doped Si substrates filled by vertically aligned carbon nanotubes (VACNTs). As a result, Co-Cu electrodes were found to have the highest charge storage capacity of 230 mC cm^{-2} among the tested composites.

2. EXPERIMENTAL PROCEDURE

2.1. VACNT Preparation

DC-PECVD (direct current – plasma enhanced chemical vapor deposition) was used to prepare VACNTs over a 1 cm^2 silicon wafer cleaned by standard RCA #1 (NH_4OH:H_2O_2:H_2O with a ratio of 1:1:5) solution and covered by a thin 7 nm Ni layer coated by an electron beam evaporation system (Veeco Co, USA). Samples were placed in the DC-PECVD chamber evacuated to a base pressure of 10 mTorr and heated up to 700 °C. A DC-plasma of hydrogen gas was used to bombard the Ni layer to form nano Ni islands (power= 1.5 W cm^{-2}, H_2 flow= 20 SCCM, time = 5 min, pressure = 2 Torr). These Ni islands would be catalysts for CNTs growth procedure. A Vertical electric field inside a mixture of H_2 and C_2H_2 plasma facilitated the growth of CNTs perpendicular to the wafer surface at Ni particles spots (H_2:C_2H_2 = 4:1, power = 2 W cm^{-2}, time = 40 min). Therefore produced CNTs are called VACNTs. VACNTs were removed out of the chamber after system cooling down.

2.2. Composite Formation

In order to cover VACNTs by metal oxide composites, they were first cleaned by soaking for 12 h into a solution of H_2SO_4 and HNO_3 with 3:1 volumetric ratio. Then the samples were washed by water several times. Nitrate precursors were used for thermal decomposition in a chamber to produce all desired composites with different 1:1 mole ratios between metal ions. In this regard, 1 M $Ni(NO_3)_2$, $Cu(NO_3)_2$ and $Co(NO_3)_2$ aqueous solutions with 1:1 and 1:1:1 mole ratios, for binary and ternary composites, respectively, were prepared and dripped over the VACNT substrate using the micro syringe method. Afterward, the samples were left in an oven for 12 h at 50 °C to dry and taken out after that for calcination in the atmospheric pressure and high temperature of 300 °C for 1 h. In this article, on the surface of a VACNT layer as a substrate electrode, we produced Ni-Co, Co-Cu and Ni-Cu binary oxides and compared them to ternary Ni-Co-Cu oxides. No more supportive materials were used on the working electrode. Mass of Silicon wafers covered by the VACNT layer was measured before deposition of the metal oxides and compared with the final composite samples. This difference is considered as the metal oxides weight and was 0.18, 0.19, 0.18 and 0.19 mg, for Ni-Co, Co-Cu, Ni-Cu and Ni-Co-Cu oxide/VACNT electrodes respectively.

3. CHARACTERIZATION

The physical appearance of produced materials was observed by a field emission scanning electron microscope (Hitachi S4160) and transmission electron microscope (TEM, Philips CM-30). Materials composition over the substrate surface was characterized by XRD (Philips Xpert pro) using Cu-kα radiation, respectively. Electrochemical properties of electrodes in an aqueous 0.5 M NaOH electrolyte were measured using galvanostatic charge-discharge and cyclic voltammetry by a standard 3-electrode cell setup (Autolab PGSTAT 30, platinum sheet

and SCE electrode were used as the counter and reference electrode respectively).

4. RESULTS AND DISCUSSION

In fact, VACNTs are hollow structures consisted of multiple concentric cylindrical carbon walls with different diameters aligned in the vertical direction perpendicular to the surface. A produced CNT with an empty space in the middle with the surrounding walls is clear in its TEM image in Figure 1(f). VACNTs have a high electrical conductivity and have a high specific surface area property due to their high aspect ratio besides its film is used as a substrate for the electrodes composite investigation. VACNT film covered a 1cm*1cm n-doped silicon wafer with an average length and diameter close to 3 μm and 100 nm respectively (Figure 1(e)).

VACNT electrical properties depend on their atomic network configuration but in produced multi-wall carbon nano tubes nickel impurities can be found that makes them good conductive materials anyway. Therefore the substrate was considered as an electrode. The important feature of CNTs in this research is their alignment and high specific surface area that they provide as a storage material for electrical charges. To compare ternary and binary composite materials over such substrates, Ni-Co, Ni-Cu, Co-Cu, and Ni-Co-Cu composite covered carbon nanotube films uniformly as are shown in Figure 1(a-d) respectively.

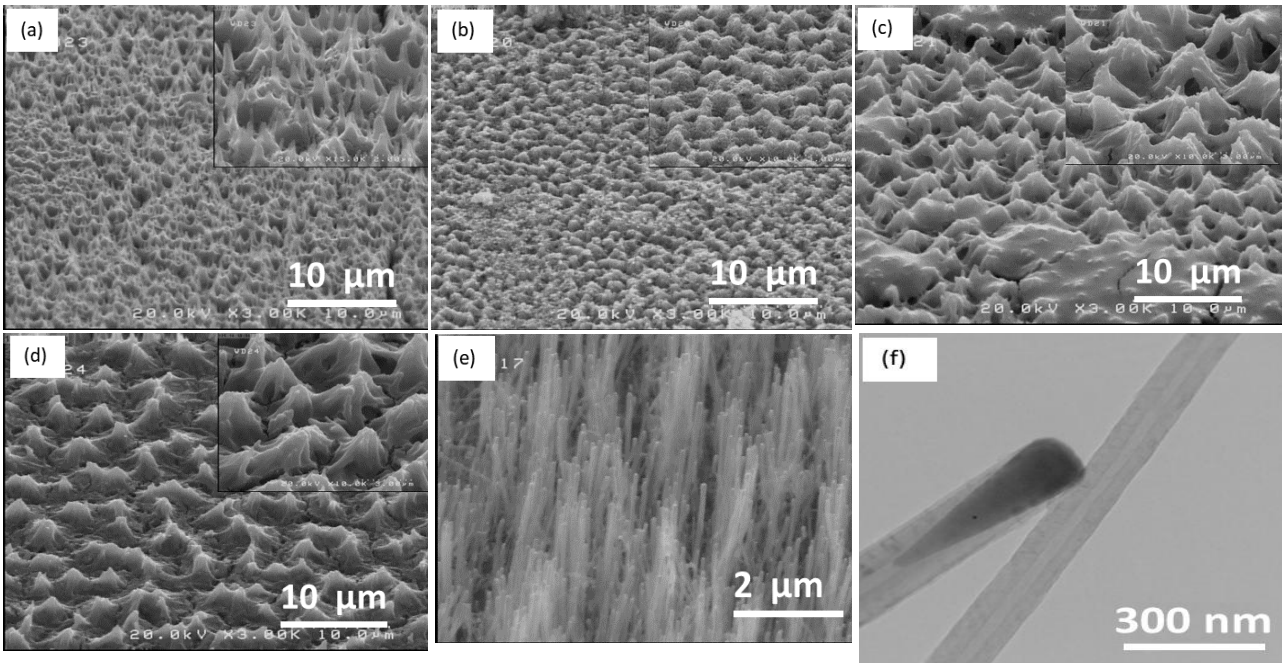

Figure 1. *FESEM images of (a) Ni-Co oxide/VACNT, (b) Ni-Cu ox ide/VACNT, (c) Co-Cu oxide/VACNT, (d) Ni-Co-Cu oxide/VACNT, (e) VACNT as 3D substrate electrode and (f) TEM image of VACNT electrode.*

TEM images were taken from Ni-Co-Cu oxide/VACNT samples before and after electrochemical experiments and proved successful and stable deposition of nano particles of metal oxides on VACNTs (Figure 2). No visible or measureable changes were observed before and after the three-electrode cell experiments of 1000 cycles that reveals appropriate binding between the metal oxide nanoparticles and

the VACNT substrate. To prepare samples for TEM, they were gently scratched by a tweezer over a carbon grid to collect VACNTs falling from the samples.

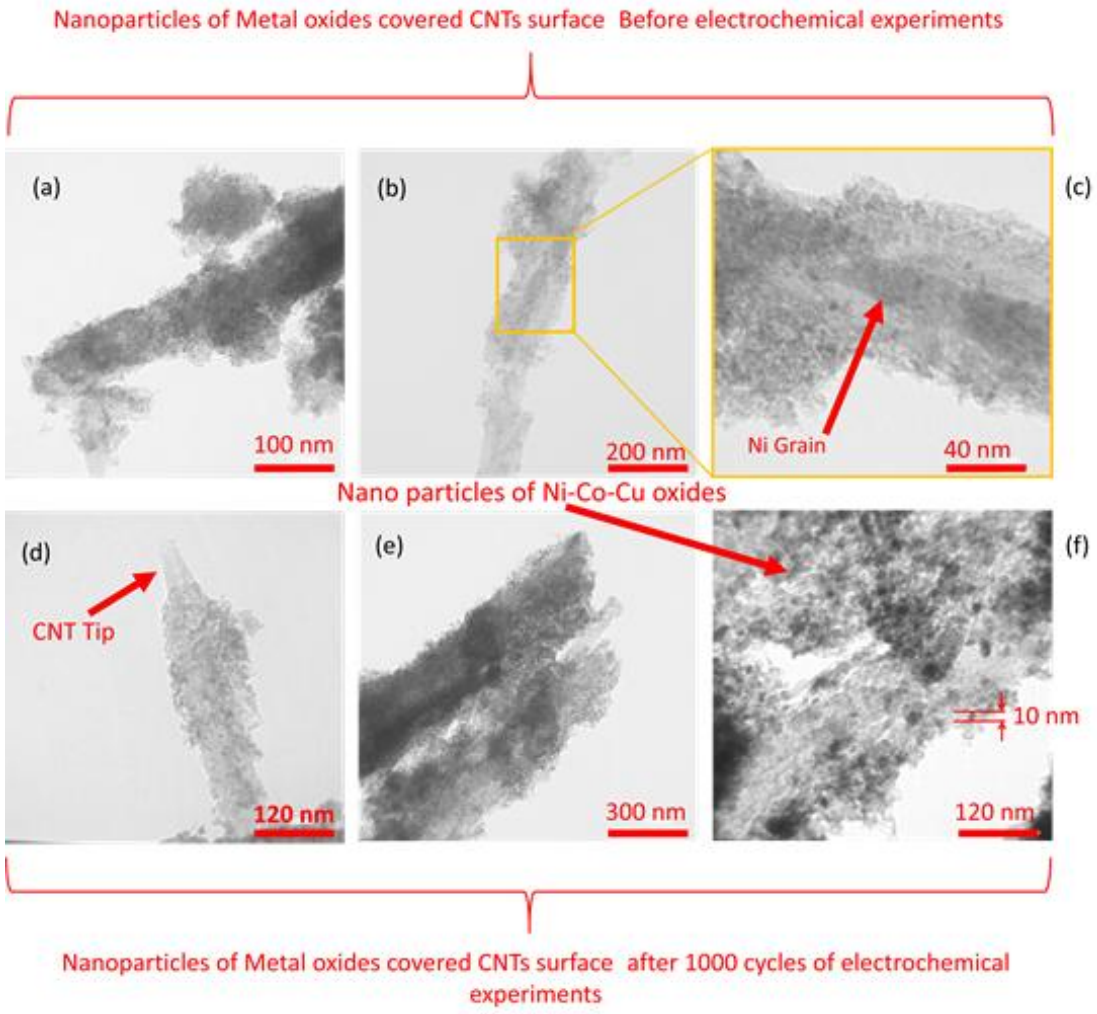

Figure 2. *TEM images of VACNTs covered by Ni-Co-Cu oxides (a-c) before and (d-f) after 1000 cycles of electrochemical experiments. Beam-like structures beneath the nano-textured material is related to CNTs while tip of a CNT is observable in (d) as well as Ni grains residual from the CNTs growth procedure. High magnification images reveals that the Ni-Co-Cu oxide is consisted of grains as tiny as 10 nm shown in (f).*

According to the TEM images, oxide layers are in fact consisted of nano scale crystalline grains that have appeared darker than bare CNTs (Figure 1(f)) which is a result of amorphous structure of the produced CNTs.

XRD patterns of binary and ternary composite electrodes are shown in Figure 3(a). XRD pattern of Ni-Co oxide/VACNT electrode contains two peaks at 2θ values of 37.2° and 45.5° corresponding to Co_3O_4 and NiO crystalline structure indicating the mixed composition of the electrode according to J-CPDS card, no 009-0418 and 075-0197, respectively. 2θ values of 36.5° and 38.8° related to CuO and 37.6° associated with Co_3O_4 were found in CO-Cu oxide/VACNT electrodes XRD pattern as well as a peak at 43° that could be attributed to Cu_2O bonds according to J-CPDS card,

no 075-1531. Ni-Cu oxide/VACNT electrode XRD pattern contained peaks at 36.7° and 38.8° for CuO and 42.7° for NiO revealing the composition of materials in the electrodes. Ni-Co-Cu oxide/VACNT electrode peaks compared to other binary composite electrodes reveals incorporation of all three metal oxide ions in the electrode structure. These peaks are a combination of peaks already were found in binary XRD patterns: 36.7° and 38.8° for CuO, 37.2° for Co_3O_4 and 42.7° for NiO electrodes.

According to the XRD results of bare VACNT samples grown in our laboratory, they have an amorphous peak around 26 degree in association with 3.42nm d-spacing that is masked by other materials in electrodes with oxide composites [19]. As a result of poor crystalline properties of our particular CNTs, we think their peaks are covered by crystalline active materials. Porous structure of CNTs in comparison with metal oxides were seen before in their TEM images where the CNTs were seen in a gray color while crystalline nanoparticles were darker significantly (Figure 2). This means that we don't expect to see peaks related to carbon atoms in XRD results, nevertheless this doesn't affect the performance of our electrodes because they are still highly conductive and porous.

Raman spectra of Ni-Co-Cu oxide/ VACNT electrodes are compared with VACNT electrodes in Figure 3(b). Two peaks in the VACNT electrode Raman spectrum exist at 1316 and 1596 cm^{-1} which are attributed to D and G-bands between carbon atoms in CNTs structure, respectively. D-bands intensity (ID) indicates sp3-bands formation among carbon atoms while G-bands intensity (IG) designates sp2-bands presence related to the graphene-mode. ID to IG ratio is shown for each Raman spectrum specifying defects reduction in composite electrodes due to treating CNTs porous surface by composite materials and removing defects as ID/IG is decreased from 1.51 to 1.09. Peaks lower than D and G-bands were found at 459, 572 and 866 cm^{-1} could be assigned to vibrational modes of Co, Cu and Ni metal oxides [28-30].

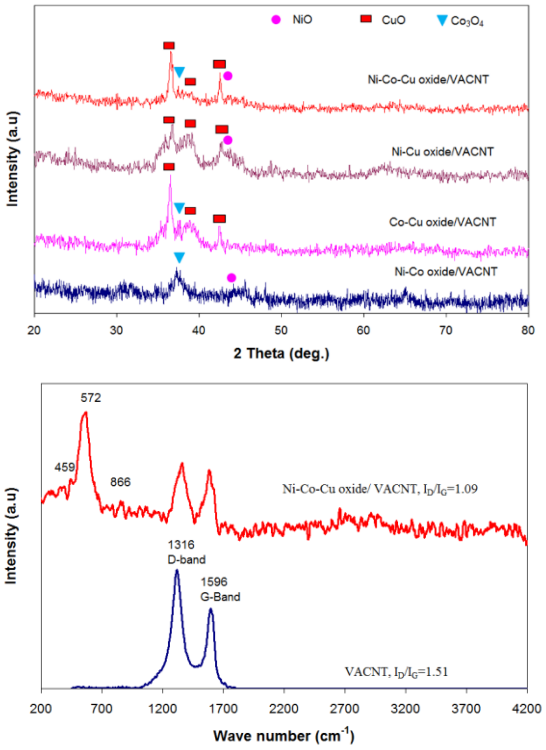

Figure 3. *(a) XRD patterns of electrodes (b) Raman spectra of VACNT and Ni-Co-Cu oxide/VACNT composite electrode.*

Different electrodes CVs are plotted in Figure 4 for scan rates of 10, 20, 30, 50, 70, 100, 150 and 200 mV and a potential window between -0.5 to 0.5 V. Figure 4(a-d) diagrams are corresponding to binary and ternary composite electrodes while Figure 4(e) represents bare VACNT electrodes CV. Different electrodes CVs are overlaid in Figure 4(f) for comparison at the 50 mv scan rate. Oxidation-reduction peaks are visible for all electrodes and stronger for electrodes with a composite due to the following redox reactions [31]:

$$NiO + OH^- \Leftrightarrow NiOOH + e^- \quad (1)$$

$$Co_3O_4 + H_2O + OH^- \Leftrightarrow 3CoOOH + e^- \quad (2)$$

$$Cu_2O + 2OH^- \Leftrightarrow 2CuO + H_2O + 2e^- \quad (3)$$

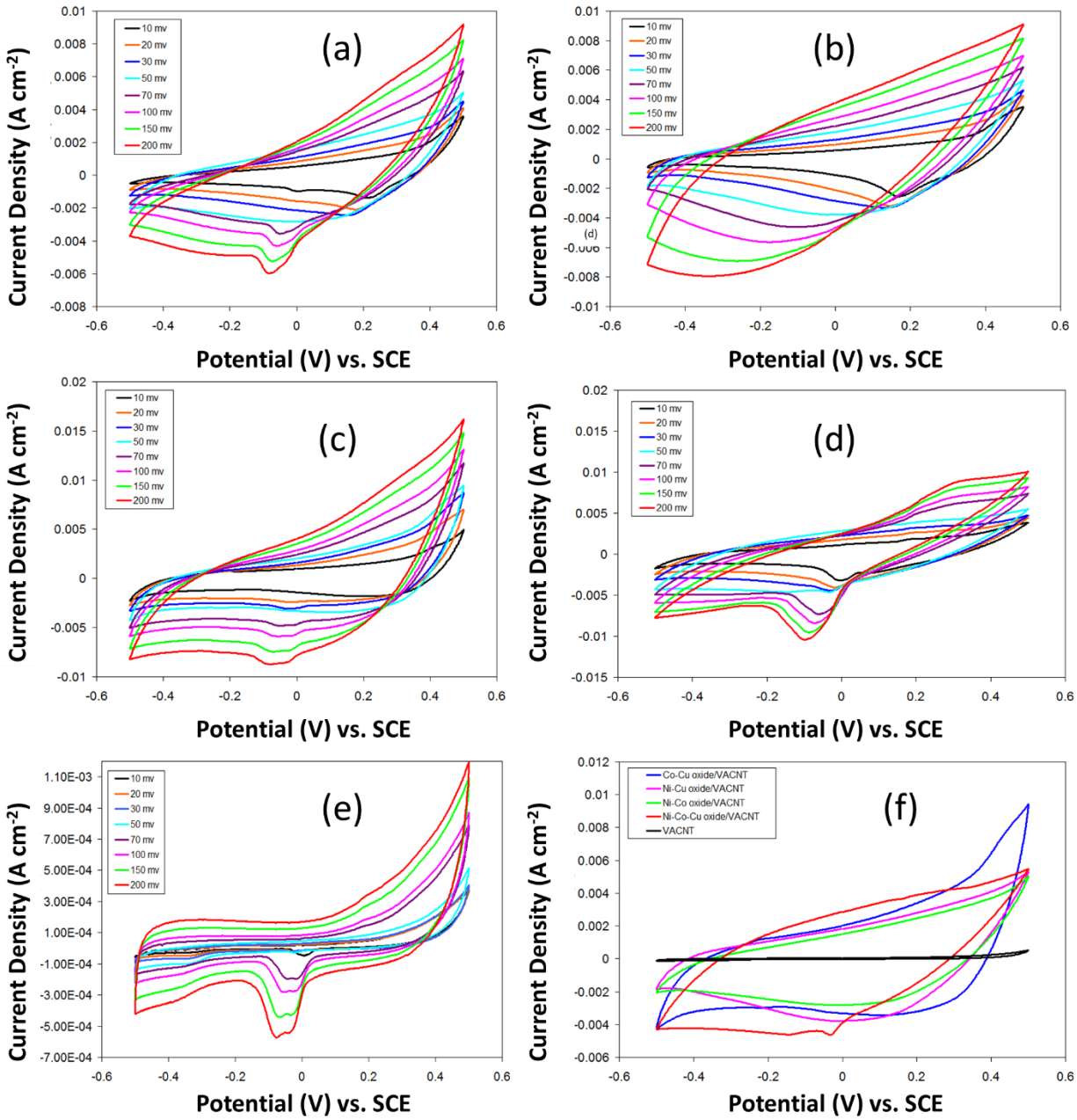

Figure 4. *CVs of (a) Ni-Co oxide/VACNT, (b) Ni-Cu oxide/VACNT, (c) Co-Cu oxide/VACNT, (d) Ni-Co-Cu oxide/VACNT, (e) VACNT electrodes at 10 up to 200 mV/s scan rate. (f) Comparison of electrodes at 50 mV/s.*

These faradic redox reactions occur at the interface of every electrode with respect to the consisting materials in that electrode and determine the charge storage capacity of the electrodes. To find the charge storage capacity of electrodes, every single chart is used for calculations. The surrounded area inside every plotted chart divided by the scan rate identifies the stored charge of the electrode:

$$Q_s = \frac{\oint I\, dV}{S_m} \qquad (4)$$

Where Sm stands for the scan rate and $\oint I\,dV$ returns the encircled area in CV charts. The area inside the VACNT electrode CV is negligible in comparison with other electrodes in Figure 4(f) therefore composite electrodes Qs has been augmented significantly as Qs is directly proportional to $\oint IdV$. Co-Cu oxide/VACNT and Ni-Co-Cu oxide/VACNT electrodes seem to have a higher capacity rather than other composite electrodes which is discussed deeper in Figure 5.

The calculated capacity of charges by Eq. 4 are plotted for all electrodes versus scan rates from 10 to 200 mV s^{-1} in Figure 5(a). The storage capacity of electrodes is decreased due to insufficient redox reactions in higher scan rates and electrolyte ions mobility limitation for transfer to electrodes surface. Maximum measured capacity was 230 mC cm^{-2} for the Co-Cu oxide/VACNT electrode at the scan rate of 10 mV. The Co-Cu/VACNT electrode capacity for charges in scan rates 10, 20, 30, 50, 70, 100, 150 and 200 mV was equal to 226, 162, 130, 96, 81, 66, 53 and 45 mC cm^{-1}. Besides Co-Cu oxide/VACNT capacity was higher than other electrodes at all scan rates. Ternary Ni-Co-Cu oxide/VACNT electrode capacity was approximately equal to the Co-Cu oxide/VACNT electrode at low scan rates but the capacity difference between Ni-Co-Cu oxide/VACNT and Co-Cu oxide/VACNT electrodes increased at higher scan rates. The Co-Cu oxide/VACNT electrode capacity for charges in similar scan rates was 212, 156, 127, 91, 66, 50, 34 and 26 mC cm^{-1}. Ni-Co oxide/VACNT electrode capacity was less than other composite electrodes in all scan-rates but charge capacity is orders of magnitude larger than bare VACNT electrodes.

Cycling life is a main parameter that determines the practical applications of any storage devices such as supercapacitor and batteries. Figure 5(b) shows electrodes capacity retention varies versus cycle numbers which is noticeable.

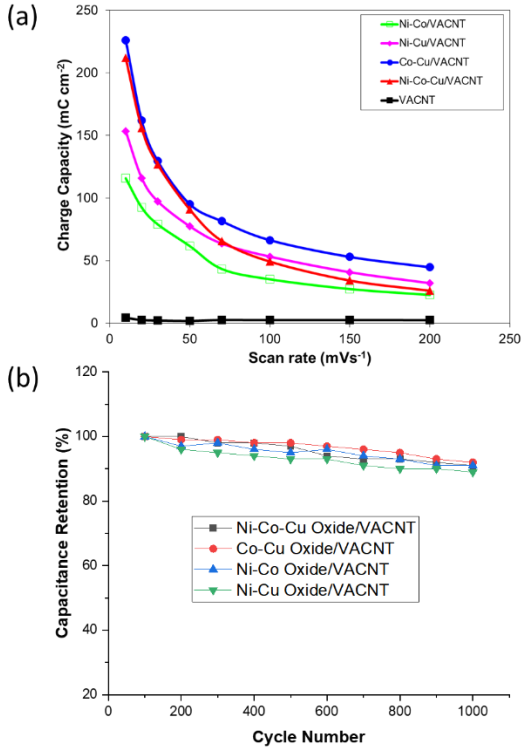

Figure 5. *(a) Capacitance dependence of composite electrodes as a function of scan rate from 10 to 200 mVs^{-1}. (b) Variation of the capacity retention of electrodes as a function of cycle number.*

As one can see in this Figure, after 1000th continuous cycles, the specific capacity was calculated to be 92%, 91%, 89% and 91% of the initial capacity for Co-Cu, Ni-Co, Ni-Cu and Ni-Co-Cu oxide/VACNT electrodes, respectively.

Electrical impedance spectroscopy (EIS) is a powerful indicator of energy storages electrochemical behavior particularly after the electrodes surface modification. All electrodes EIS results in a 1 M KOH aqueous solution with 5 mV AC stimulation voltage are shown in Figure 6 where magnitude and phase angle are plotted separately in Figure 6(a, b) and the Nyquist plot of impedance is presented in Figure 6(c)

for 0.1 to 100000 Hz frequencies. An equivalent electrical circuit shown in Figure 6(c) is considered to model EIS plots and behavior of the electrodes. Every electrode parameters are derived using the Z view program and is provided in Table 1. Equivalent models are compared with the EIS results in Figure 7. According to the fitting accuracy observed there, the considered model is believed to be efficiently reliable. The equivalent circuit consists of an open circuit type of the Warburg element (W_o) in series with a resistance (R_{ct}) while both are parallel to a capacitor (C). Finally, this combination of elements are in series with a resistance (R_s). Impedance of open circuit type of Warburg elements (ZW_o) is ruled by the Equation 5.

$$Z_{Wo} = Wo_r \times \frac{\coth([j.\omega.Wo_T]^{Wo_p})}{[j.\omega.Wo_T]^{Wo_p}} \quad (5)$$

Warburg element is significant in low frequencies and is detected by the Nyquist plot finite slope (~45°). This element models diffusion behavior of ions alongside Rct. Rct is called charge transfer resistance and is responsible to model electrons transfer to electrodes metallic materials by ions movement and diffusion. Obviously, such process is dependent on parameters such as concentration and temperature [32]. A semicircle shape in high frequencies of the Nyquist plot indicates charge transfer capability of electrodes represented by Rct that is proportional to its curvature diameter. Diffusion phenomena is a slow process and is controlled by the electrodes pores properties. Therefore, their effects are visible in Nyquist plots low frequencies. All electrodes have had a small R_{ct} that could be related to the electrodes highly porous structure while larger Warburg elements impedance magnitude could be a reason of electrodes resistivity against the mass transfer [2]. A zoomed in Figure of the Nyquist plot in high frequencies is inserted in Figure 6(c) as well as in Figure 7. According to these Figures, the Co-Cu oxide/VACNT electrode, particularly, have had a semi-circle curvature in their high frequencies which somewhat, diminishes in other electrodes that could be a reason of charge transfer conductivity enhancement [4]. Impedance magnitude drop confirms capacitive properties of electrodes until it remains constant at high frequencies which reveals electrodes internal resistance R_s. R_s is proportional to the electrodes inner resistance and electrolyte anionic characteristics and could be calculated by measuring electrodes impedance magnitude in high frequencies that the phase angle has dropped to zero approximately. More accurate results for R_s are provided in Table 1 that constant similar resistance in all samples in high frequencies shows all electrodes have had a similar electrolyte resistance. On the other hand, in low frequencies, phase angles of all electrodes are closer to capacitors ideal phase angle i.e. -90º which is shown in Figure 6(b) and is an indicator of the electrodes capacitive properties.

4. CONCLUSIONS

Co-Cu, Ni-Co, Ni-Cu and Ni-Co-Cu oxides were successfully produced by a thermal decomposition method to coat

Table 1. *Electrodes equivalent electrical circuit parameters.*

Electrodes	Rs (Ω)	Rct (Ω)	C (μF)	Wor (Ω)	Wot $(rad.s)^{-1}$	Wop
Ni-Co	2.50	0.487	456.	11.22	0.09524	0.325
Co-Cu	2.31	0.797	219	12.33	0.46	0.379
Ni-Cu	2.04	0.741	308.	2.33	0.00759	0.303
Ni-Co-Cu	3.07	0.730	959.	0.30	0.00107	0.326

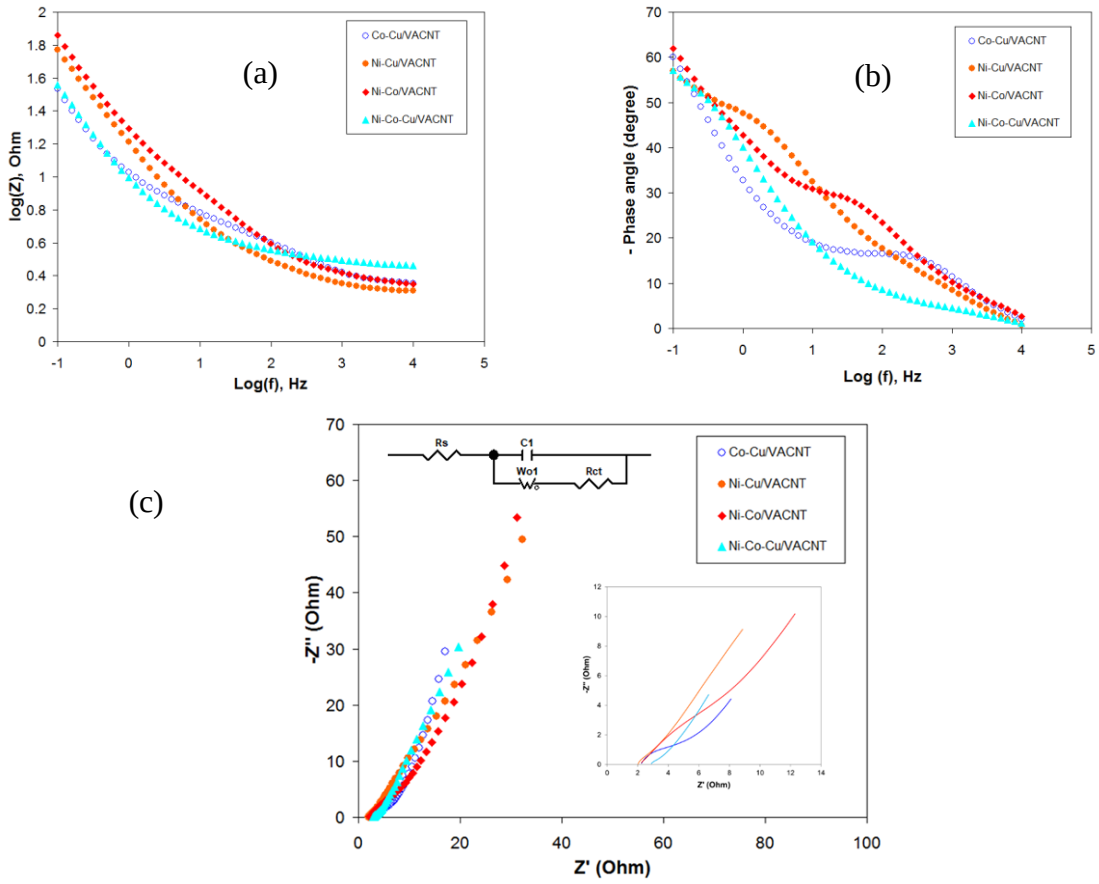

Figure 6. *Impedance spectroscopy plots of electrodes at 10000 to 0.1 Hz sweep. (a) Magnitude, (b) phase and (c) Nyquist diagram of EIS results are depicted for every electrode. The Equivalent proposed circuit is shown in (c). Insert in (c) is a zoomed in version of the nyquist diagram in high frequencies to demonstrate their high frequency characteristics better.*

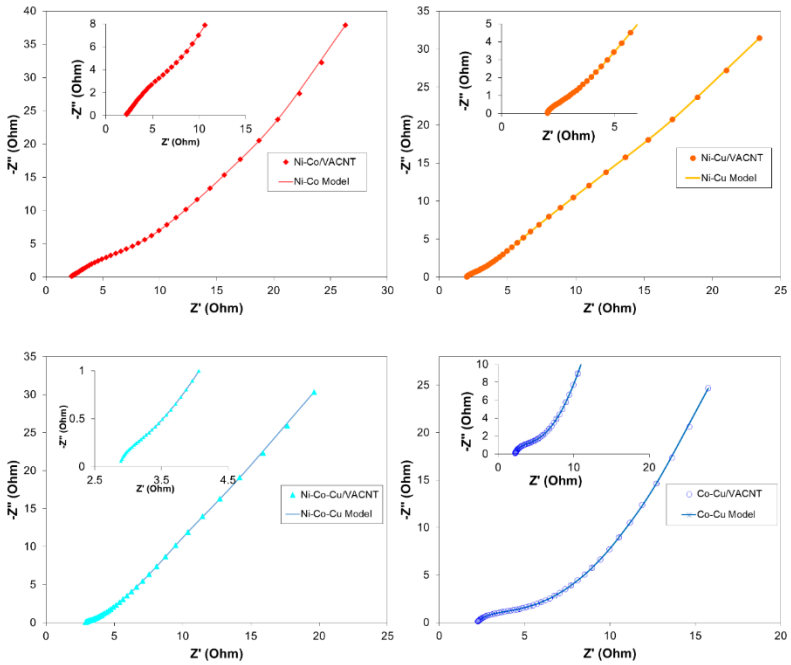

Figure 7. *Accuracy of the fitted equivalent circuit parameters to the real experimental results. Solid lines are related to the equivalent model and markers show the actual measured impedance.*

VACNT structures over a silicon wafer substrate as electrodes for aqueous energy storages. The charge capacity of produced electrodes was measured by cyclovoltammetry technique and Co-Cu oxide/VACNT composite found to have the largest charge capacity of 230 mC cm^{-2} in a scan rate of 10 mV and 1 V potential window. Ni-Co-Cu/VACNT composite materials had a high capacity for electrical charges but it wasn't higher than the binary Co-Cu/VACNT composite electrode. Therefore the Co and Cu oxides composite was more efficient as an active material for energy storage devices.

ACKNOWLEDGEMENT

The financial support of this work by the Research Council of the Imam Khomeini International University and Iran Nanotechnology Initiative Council is gratefully acknowledged.

REFERENCES

1. Saengchairat, N., Tran, T., Chua, C.-K., (2017). "A review: Additive manufacturing for active electronic components", *Virtual Physical Prototyping*, 12: 31-46.
2. Jokar, E., Shahrokhian, S., (2015). "Synthesis and characterization of NiCo 2 O 4 nanorods for preparation of supercapacitor electrodes", *Journal of Solid State Electrochemistry*, 19: 269-274.
3. Mohammad-Rezaei, R., Razmi, H., (2016). "Preparation and characterization of reduced graphene oxide doped in sol-gel derived silica for application in electrochemical double-layer capacitors", *International Journal of Nanoscience*, 12: 233-241.
4. Wessells, C. D., et al., (2011). "Nickel hexacyanoferrate nanoparticle electrodes for aqueous sodium and potassium ion batteries", *Nano letters*, 11: 5421-5425.
5. Chen, Y., et al., (2013). "Synthesis of carbon coated Fe3O4/SnO2 composite beads and their application as anodes for lithium ion batteries", *Materials Technology*, 28: 254-259.
6. Huang, F., et al., (2011). "Nanosized Zn–Sn metal composite oxide: a new anode material for Li ion battery", *Materials Science and Technology*, 27: 29-34.
7. Khorasani-Motlagh, M., Noroozifar, M., Yousefi, M., (2011). "A simple new method to synthesize nanocrystalline ruthenium dioxide in the presence of octanoic acid as organic surfactant", *International Journal of Nanoscience Nanotechnology*, 7: 167-172.
8. Zhang, S., Chen, G. Z., (2008). "Manganese oxide based materials for supercapacitors", *Energy Materials*, 3: 186-200.
9. Purushothaman, K., et al., (2017). "Design of additive free 3D floral shaped V2O5@ Ni foam for high performance supercapacitors", *Materials technology*, 32: 584-590.
10. Liu, Y., et al., (2013). "Graphene and nanostructured Mn3O4 composites for supercapacitors", *Integrated Ferroelectrics*, 144: 118-126.
11. Tan, D. Z. W., et al., (2014). "Controlled synthesis of MnO2/CNT nanocomposites for supercapacitor applications", *Materials Technology*, 29: A107-A113.
12. Jiang, X., et al., (2018). "Facile preparation of a novel composite Co-Ni (OH) 2/carbon sphere for high-performance supercapacitors", *Materials Technology*, 1-9.
13. Hosseini, M., et al., (2015). "Study of super capacitive behavior of polyaniline/manganese oxide-carbon black nanocomposites based electrodes", *International Journal of Nanoscience Nanotechnology*, 11: 147-157.
14. Zhang, Z., et al., (2016). "Mental-organic framework derived CuO hollow spheres as high performance anodes for sodium ion battery", *Materials Technology*, 31: 497-500.
15. Moosavifard, S. E., et al., (2014). "Facile synthesis of hierarchical CuO nanorod arrays on carbon nanofibers for high-performance supercapacitors", *Ceramics International*, 40: 15973-15979.
16. 16. Prasad, K. P., et al., (2011). "Fabrication and textural characterization of nanoporous carbon electrodes embedded with CuO nanoparticles for supercapacitors", *Science and Technology of Advanced Materials*, 12: 044602.
17. Kim, T., et al., (2016). "Synthesis and characterization of NiCo2O4 nanoplates as efficient electrode materials for electrochemical supercapacitors", *Applied Surface Science*, 370: 452-458.
18. Zhang, J., et al., (2015). "Flower-like nickel–cobalt binary hydroxides with high specific capacitance: Tuning the composition and asymmetric capacitor application", *Journal of Electroanalytical Chemistry*, 743: 38-45.
19. Saghafi, M., et al., (2015). "Preparation of Co-Ni oxide/vertically aligned carbon nanotube and their electrochemical performance in supercapacitors", *Materials and Manufacturing Processes*, 30: 70-78.
20. Liu, X., et al., (2016). "Facile synthesis of Cu3Mo2O9@ Ni foam nano-structures for high-performance supercapacitors", *Materials Technology*, 31: 653-657.

21. Wang, R., et al., (2017). "Nanoporous Cu/Co alloy based Cu2O/CoO nanoneedle arrays hybrid as a binder-free electrode for supercapacitors", *Journal of Materials Science: Materials in Electronics*, 28: 8755-8763.
22. Tang, Y.-L., Hou, F., Zhou, Y., (2016). "Preparation and electrochemical performances of Coχ Ni (1− χ)(OH) 2 coated carbon nanotube free standing films as flexible electrode for supercapacitors", *Materials Technology*, 31: 377-383.
23. Yin, J., Park, J. Y., (2014). "Electrochemical investigation of copper/nickel oxide composites for supercapacitor applications", *International Journal of Hydrogen Energy*, 39: 16562-16568.
24. Nwanya, A. C., et al., (2017). "Nanoporous copper-cobalt mixed oxide nanorod bundles as high performance pseudocapacitive electrodes", *Journal of Electroanalytical Chemistry*, 787: 24-35.
25. Zhang, L., Gong, H., (2017). "Unravelling the correlation between nickel to copper ratio of binary oxides and their superior supercapacitor performance", *Electrochimica Acta*, 234: 82-92.
26. Fu, H., et al., (2015). "Electrochemical deposition of mesoporous NiCo2O4 nanosheets on Ni foam as high-performance electrodes for supercapacitors", *Materials Research Innovations*, 19: S255-S259.
27. Wu, C., et al., (2017). "Hybrid Reduced Graphene Oxide Nanosheet Supported Mn–Ni–Co Ternary Oxides for Aqueous Asymmetric Supercapacitors", *ACS applied materials & interfaces*, 9: 19114-19123.
28. Kim, N.-I., et al., (2016). "Enhancing activity and stability of cobalt oxide electrocatalysts for the oxygen evolution reaction via transition metal doping", *Journal of The Electrochemical Society*, 163: F3020-F3028.
29. Xu, Y.-T., et al., (2015). "Co-reduction self-assembly of reduced graphene oxide nanosheets coated Cu2O sub-microspheres core-shell composites as lithium ion battery anode materials", *Electrochimica Acta*, 176: 434-441.
30. Zhang, J., et al., (2018). "Synthesis of 3D porous flower-like NiO/Ni_6 MnO_8 composites for supercapacitor with enhanced performance", *Journal of Materials Science: Materials in Electronics*, 29: 7510-7518.
31. Pawar, S. M., et al., (2016). "Multi-functional reactively-sputtered copper oxide electrodes for supercapacitor and electro-catalyst in direct methanol fuel cell applications", *Scientific reports*, 6: 21310.
32. Sekar, N., Ramasamy, R. P., (2013). "Electrochemical impedance spectroscopy for microbial fuel cell characterization", *J Microb Biochem Technol S*, 6: 12-23.